

# Broadband 10–300 GHz stimulus-response sensing for chemical and biological entities

Min Ki Choi, Kimberly Taylor, Alan Bettermann  
and D W van der Weide

Department of Electrical & Computer Engineering, University of Wisconsin-Madison,  
1415 Engineering Drive, Madison, WI 53706-1691 USA

Received 1 March 2002

Published 17 October 2002

Online at [stacks.iop.org/PMB/47/3777](http://stacks.iop.org/PMB/47/3777)

## Abstract

By illuminating the sample with a broadband 10–300 GHz stimulus and coherently detecting the response, we obtain reflection and transmission spectra of common powdered substances, and compare them as a starting point for distinguishing concealed threats in envelopes and on personnel. Because these samples are irregular and their dielectric properties cannot be modulated, however, the spectral information we obtain is largely qualitative. To show how to gain quantitative information on biological species at micro- and millimetre-wave frequencies, we introduce thermal modulation of a globular protein in solution, and show that changes in single-wavelength microwave reflections coincide with accepted visible absorption spectra, pointing the way towards gaining quantitative chemical and biological spectra from broadband terahertz systems.

## 1. Introduction

With the advent of short-pulse coherent measurement techniques, either based on optoelectronic or purely electronic means of generating and detecting broadband radiation, researchers are now equipped with new tools for qualitative sensing and even quantitative measurement of chemical and biological entities. The possibility of using stand-off (i.e. non-contact stimulus/response measurements at a distance) techniques to assess the presence of chemical and biological weapons is of particular interest, and is an application that is well-suited to wavelengths at the millimetre length scale, since these can penetrate clothing and envelopes while still forming images with useful spatial resolution.

Hence, this recent interest in sensing chemical and biological entities with frequencies in the megahertz through terahertz regime has brought about a growing body of experimental results, as well as raising curiosity about the fundamental interactions with and effects of this broadband radiation on biological samples.

Such samples can be classified by their phase—vapour, liquid or solid—as well as by their degrees of homogeneity and complexity—purified, admixture or tissue. Furthermore, the interaction of sample volume and wavelength will set limits on and complicate the interpretation of broadband measurements. Many broadband pulsed systems have <40 dB dynamic range, which limits how thick a highly-absorbing sample can be, while thin or more transparent samples will require a minimum interaction length with the radiation to produce meaningful contrast above the noise and non-repeatability of broadband systems. Because sample thickness is often commensurate with measurement wavelength, etalon effects of the sample, in which multiple quarter- or half-wave resonances modulate the detected signal, are often compounded with auxiliary standing-wave effects of the measurement apparatus and environment. While radiometric millimetre-wave techniques that rely on the sample's black-body radiation would minimize these standing wave effects, these are neither broadband systems, nor do they illuminate the sample.

Thus, in contrast with traditional spectroscopy techniques in the infrared and visible, where sample size is typically much larger than the wavelength, probing chemical and biological samples with broadband terahertz radiation requires reconsideration and careful specification of the sample's physical characteristics. The confounding effects of these characteristics on the raw result usually require a differential (normalized) measurement technique to measure the actual sample behavior, and this can result in standing wave effects being magnified.

While we briefly survey the background of broadband sensing for chemical and biological samples, our principal focus here is on sensing solid-phase, condensed samples that are either pure or admixtures of known substances, typical of what might be expected in a concealed bulk (as distinct from trace) threat.

In addition, to advance an argument for better understanding of sample/radiation interactions, we discuss microwave spectroscopy of purified biomolecules in solution, in this case a globular protein, bovine pancreatic ribonuclease A (RNase A), which we thermally denature (unfold) while simultaneously probing the sample with microwave and visible light. In this experiment, we gain two important advantages:

- We can externally modulate the sample (in this case the protein's conformation).
- We can independently confirm our microwave measurement with an accepted optical technique.

Such modulation and independent, simultaneous confirmation is usually lacking in broadband measurements, and this makes interpretation of the data more challenging.

Since, on the other hand, concealed threats are (almost by definition) not amenable to modulation, single-line or narrowband radiation is probably less useful for qualifying the nature of the threat than is broadband radiation. Although it has more power, and microwave holography has been reported for imaging of concealed weapons (Sheen *et al* 2001), narrowband illumination fundamentally restricts the availability of spectral information in a complex environment. Even with the richer spectrum of broadband radiation, however, not having independent confirmation of contrast mechanisms (such as an optical spectroscopic probe) leaves us with few choices other than to look for characteristic patterns in the broadband reflection or transmission spectra that we measure. The coherence of these synchronous generation/detection spectrometers enables us to measure both magnitude and phase of transmission and reflection, and while a characteristic spectral pattern can emerge in the phase spectrum, there is still more progress to be made in quantifying these spectra.

Nonetheless, having millimetre-scale spatial resolution and GHz-level spectral resolution enables qualitative identification of features that, in a pattern-matching algorithm, can be applied to a form of spectroscopic imaging for security screening. Thus the main results

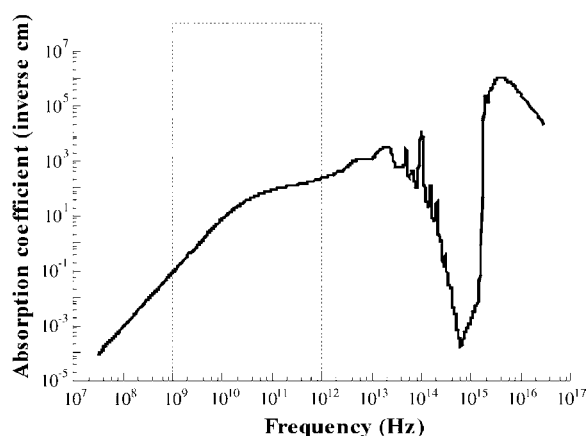


**Figure 1.** Absorption coefficient of liquid water at 20 °C highlighting the terahertz regime (Segelstein 1981).

presented here are spectra that might be further processed by such an algorithm to result in a false-colour image that would indicate the presence of unusual (chemical or biological) substances concealed within envelopes or under clothing.

## 2. Background

Broadband microwave spectrometers or network analysers, whether time- (Feldman *et al* 1996) or frequency-domain (Hollis *et al* 1980), have been used to measure chemical and biological samples, both in bulk and attached to transducer surfaces, such as planar transmission lines (Hefti 1999, Facer *et al* 2001). While interpretation of the spectra from all but the simplest samples (e.g. pure water) has been difficult, characteristic signatures of biomolecular conformation have nonetheless been observed.

Biological macromolecules are expected to exhibit weak absorptions, if any, in the microwave and terahertz regimes. Proteins are weakly dielectric, and exhibit absorption due to orientational relaxation at radio frequencies (Pethig 1979). Double-helical DNA does not exhibit such orientational relaxation, since the dipole moments of the two helices nullify each other. Normal mode analysis predicts that both proteins (Tama *et al* 2000) and DNA (Bykhovskaia *et al* 2001) should exhibit multiple absorptions in the terahertz range due to a variety of collective, vibrational, twisting and librational modes.

All biological macromolecules, however, are surrounded by one or more shells of bound water (Pethig 1979); molecules in solution are also bounded by bulk solution. Water is a strongly dielectric molecule, with absorptions throughout the microwave and terahertz regimes (Segelstein 1981). Figure 1 shows the absorption spectrum of liquid water. Normal mode analysis predicts multiple absorptions for water in the microwave and terahertz ranges (Kindt and Schmuttenmaer 1997). Hence, the primary contributor to the absorption of any solvated biological macromolecule is water, either in bound or bulk form. The observed spectra will be a combination of absorptions from bound and/or bulk water, the biological molecule(s), and interfacial dielectric phenomena. Several authors have described responses of DNA and proteins at microwave and terahertz frequencies (Pethig 1992, Markelz *et al* 2000, Nandi *et al* 2000, Taylor and van der Weide 2001a, 2001b, Wichaidit *et al* 2001).

Cells and tissues are complex mixtures of biological macromolecules and water. Spectra from such samples are not amenable to simple analysis, but differences in hydration may

be used for imaging and/or identification purposes (Han and Zhang 2000, Smye *et al* 2001, Fitzgerald *et al* 2002).

### 3. Approach

#### 3.1. Broadband stimulus/response

We focus here on coherent broadband stimulus/response measurements, working both in reflection and in transmission. While the transmission method can be used for low-loss probing through envelopes, the reflection method can be applied generally from envelopes to the human body, which cannot be imaged in transmission with terahertz systems due to high absorption of water.

To generate energy in the 1–1000 GHz regime, we use nonlinear transmission line (NLTL) pulse generators coupled to wideband planar antennas (van der Weide *et al* 1991, 1993, Konishi *et al* 1992, Bostak 1994, Bostak *et al* 1994, Konishi *et al* 1994, Rodwell *et al* 1994). The GaAs IC NLTLs used in this work consist of series inductors (or sections of high-impedance transmission line) with varactor diodes periodically placed as shunt elements. On this structure at room temperature a fast ( $\sim 0.5$ – $2$  ps) voltage step develops from a sinusoidal input because the propagation velocity  $u$  is modulated by the diode capacitance,  $u(V) = 1/\sqrt{LC(V)}$ , where  $L$  is the line inductance and  $C(V)$  the sum of the diode and parasitic line capacitance (Rodwell *et al* 1991, 1994). Limitations of the NLTL arise from its periodic cutoff frequency, waveguide dispersion, interconnect metallization losses, and diode resistive losses. Improvements in NLTL design have resulted in sub-picosecond pulses at room temperature (van der Weide 1994).

The first electronic THz systems used resonant or broadband (bowtie) antennas driven directly by NLTLs for generation of freely propagating pulses. These pulses can be focused and collected in a manner exactly analogous to optoelectronic THz systems (Nuss and Orenstein 1998), using substrate lenses and reflective optics. For coherent detection, the pulse from the receiver's NLTL was used to drive a sampler, essentially a broadband frequency mixer, whose temporal output can be sent to an oscilloscope or Fast-Fourier Transform (FFT) spectrum analyser for display in the frequency domain.

#### 3.2. Sample preparation

To examine the content of envelopes with an eye toward distinguishing common powders from potentially dangerous ones, we prepared samples of sugar, starch, flour, and talcum powder. These were placed into petri dishes having 90 mm diameter and 20 mm height when covered. The masses of each sample were 56.6, 61.2, 62.0 and 84.6 grams for sugar, starch, flour and talcum powder, respectively, and they were used in both reflection and transmission. Additional transmission measurements were done through envelopes with the same four powders and with *B. cereus*, a simulant of *B. anthracis*.

*Bacillus cereus* (from the laboratory of Dr John Lindquist, University of Wisconsin Department of Bacteriology) was inoculated onto two tryptic soy agar plates (100 × 20 mm) as a lawn and incubated 120 h at 27 °C. The surfaces of the plates were scraped using a flat spatula to recover spores (and residual of the vegetative cells). A slurry of this material was made by diluting it 1:1 with sterile H<sub>2</sub>O. Approximately 200 mg of spore slurry was evenly spread over a 7 × 10 cm piece of standard office copier paper, which was then dried at room temperature overnight.

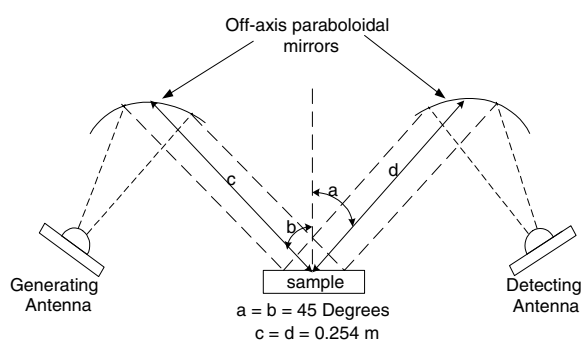


Figure 2. Reflection measurement setup.

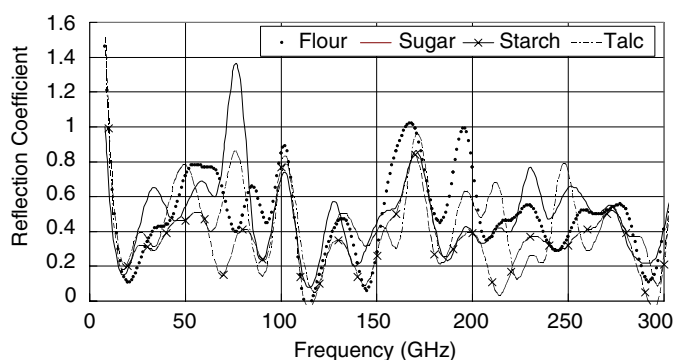


Figure 3. Normalized reflection magnitude of common powders. Standing-wave effects at  $\sim 75$  GHz cause an anomalous peak in the ratio of the sugar sample to the empty petri dish.

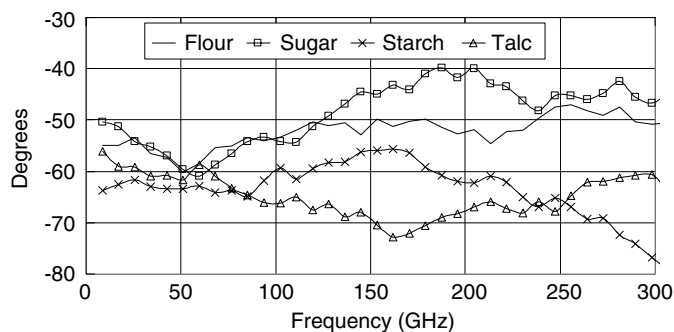


Figure 4. Normalized, unwrapped reflection phase of common powders.

### 3.3. Reflection

The reflection measurement setup is shown in figure 2. First, we used a copper plate with the same size of the samples to obtain a magnitude and phase reference. Each petri dish sample was collected and normalized to the reference values (figures 3 and 4).

For both lossy and highly conducting materials, reflection measurements are preferable since transmission may not have enough signal-to-noise. As can be seen in figure 3, the reflection magnitude shows some differences in spectral patterns, part of which can be

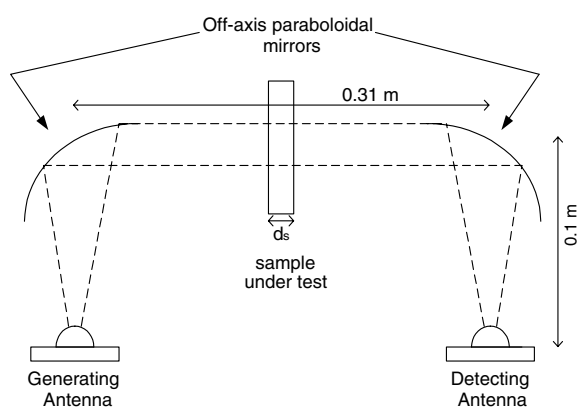


Figure 5. Transmission measurement setup diagrams: without sample.

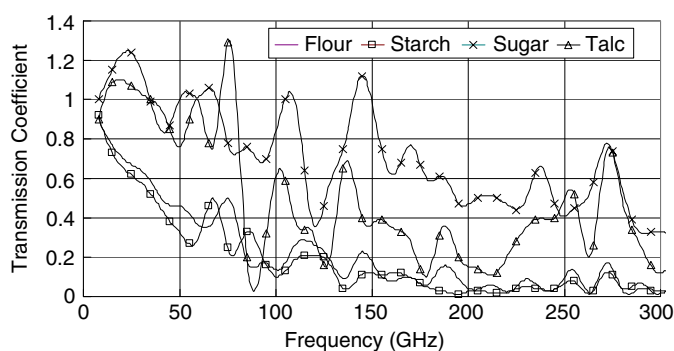


Figure 6. Normalized transmission magnitude for samples in petri dishes. Note effects of standing waves on ratios plotted.

attributed to standing waves when normalized (hence the  $> 1$  reflection coefficient magnitude). The phase information, additionally, can be used to identify the sample powders.

### 3.4. Transmission

The transmission measurement setup is shown in figure 5. Transmission through samples was normalized by the detected signal using empty containers in the beam path. We inserted Mylar resistive sheet attenuators into the beam path to check for uniform attenuation across the spectrum.

With this configuration we examined samples both in petri dishes and in sealed envelopes (figures 6–9). The normalization for the petri dishes was done by using an empty petri dish, and for the envelope measurement, the reference values were taken with an empty envelope at the sample position as in figure 5.

We expect frequency-dependent attenuation through the samples: figure 6 shows more attenuation with increasing frequency than figure 8 because the thickness of petri dishes exceeds that of the envelopes. Furthermore, reflection measurements (figure 3) do not show this  $\sim 1/f$  type of attenuation. Generally, flour and starch samples have very similar patterns in the magnitude, but they are not identical. Although not shown in the figures, a notable result

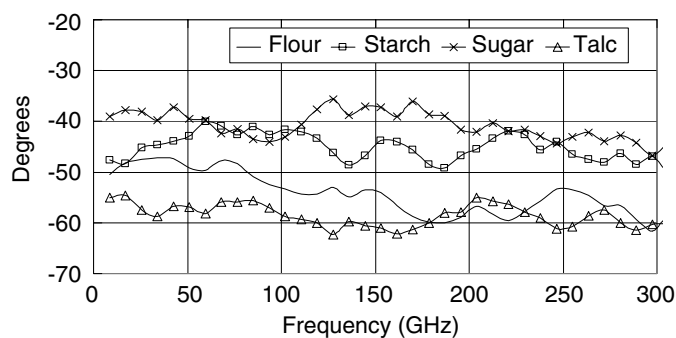


Figure 7. Normalized and unwrapped transmission phase for samples in petri dishes.

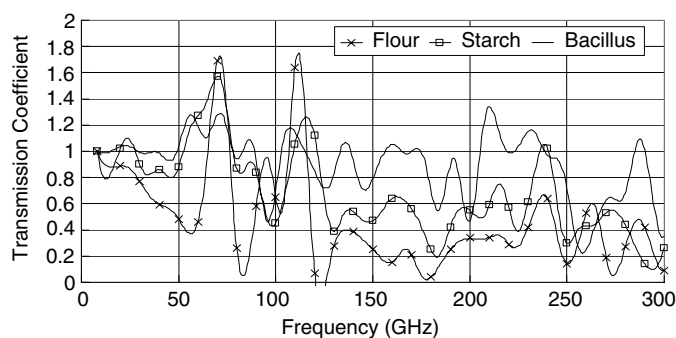


Figure 8. Normalized transmission magnitude for samples in envelopes, comparing flour, starch and *B. cereus* spores.

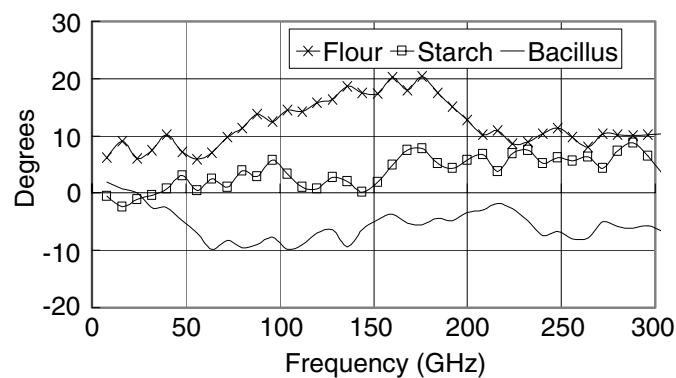
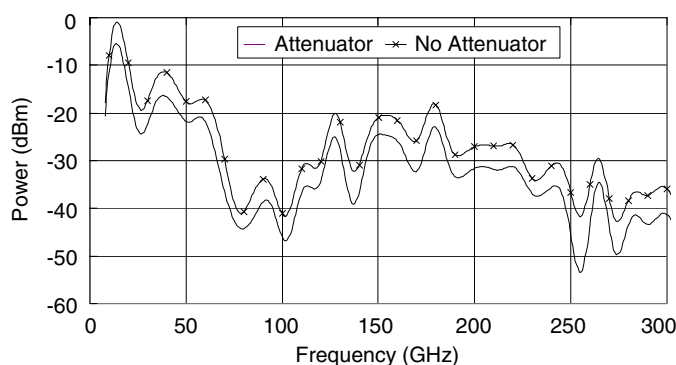


Figure 9. Normalized and unwrapped transmission phase for samples in envelopes.

is that for both petri dish and envelope samples, the attenuation for flour and starch is larger than for the others, making identification more feasible.

While the transmission magnitude through envelopes gives spectra that are difficult to distinguish, the phase signal has given a distinctive negative dispersion characteristic for the anthrax simulant. This signal, in conjunction with measuring transmission characteristics of neighbouring pixels, would provide additional information about potential threats in envelopes.



**Figure 10.** Transmission with and without a 300 ohm/square attenuating sheet.

Standing-wave effects cause the ratios plotted to have magnitudes  $> 1$  at some frequencies. Inserting attenuators into the beam path could reduce this standing wave problem, at the expense of signal-to-noise. To check for uniform attenuation, we inserted a Mylar resistive sheet (300 ohms per square) in the beam path (figure 10). The attenuation was 5 dB at most frequencies, but small variations are clear, and these are magnified when taking the ratio of two measurements.

### 3.5. Reflection from solution proteins

In order to address uncertainties in measuring microwave interactions with biomolecules, we chose a purified protein in solution whose conformation could be thermally modulated and independently verified with optical means. Bovine pancreatic ribonuclease A (RNase A), a small globular protein, was used to correlate microwave reflection measurements with changes in protein conformation. RNase A experiences reversible thermal denaturation under a variety of conditions. Conformational changes of RNase A can be detected by monitoring the UV/VIS absorbance at 278.5 nm (Klink *et al* 2000, Pace *et al* 1999). Reflection measurements from 0.5 to 6.5 GHz were performed using a resonant slot antenna (Akhavan and Mirshekar-Syahkal 1999) attached to a vector network analyzer. The slot antenna was attached to a fused quartz UV/VIS cuvette. A UV/VIS spectrophotometer could be used in conjunction with the antenna/cuvette assembly to obtain simultaneous optical and microwave measurements.

The presence of RNase A in solution could be detected using our slot antenna system. Figure 11 shows a typical spectrum of RNase A; figure 12 shows variation of the position of a single peak with protein concentration. The peak minimum increases approximately linearly with increasing protein concentration. Note that these changes are quite small, less than 0.8 GHz over a concentration range from 0 to 2.97 mg mL<sup>-1</sup>. However, this experiment demonstrates that microwave spectra are sensitive to protein concentration, as expected. This sensitivity would be expected not only for protein, but also for any solute that affects the structure of bulk water.

The response of the spectra of RNase A to increasing temperature is shown in figure 13. Note that peaks shift and broaden with increasing temperature. The upper half of figure 14 displays the response of a single peak at approximately 3.5 GHz. Note that the position of the peak minimum varies in a sinusoidal manner. Such a sinusoidal response is expected for cooperative phenomena such as protein unfolding (Creighton 1993) and is absent when buffer alone is heated under the same conditions (data not shown). This peak fitted well to a 2-state

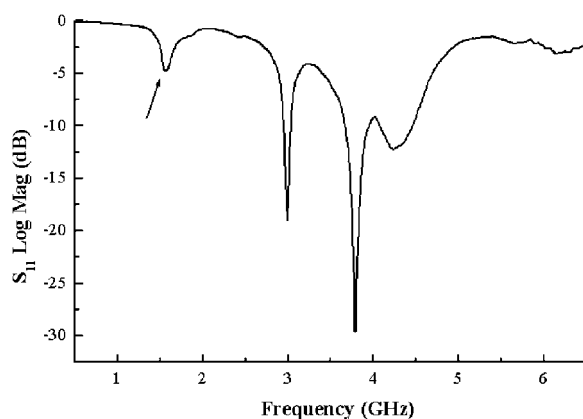


**Figure 11.** Reflection spectrum from a slot antenna affixed to a cuvette with RNase-A solution. Arrow indicates a peak that is tracked in thermal measurements.

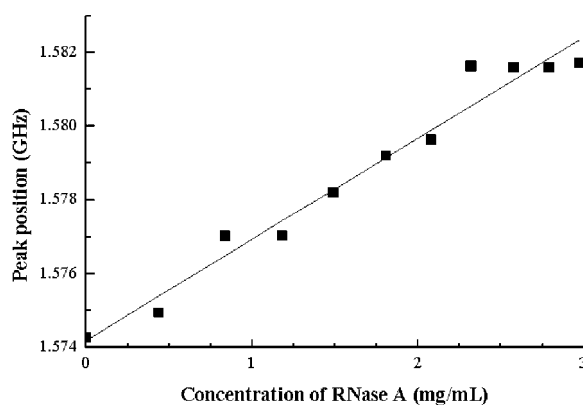


**Figure 12.** Concentration dependence of frequency shift for peak noted in figure 11.

unfolding model (Klink *et al* 2000). Results from fitting of the peak at 3.5 GHz, and from fitting to the UV/VIS data alone, are shown in the lower half of figure 14. The microwave data predicts a lower midpoint temperature ( $T_m$ ) and unfolding enthalpy ( $\Delta H_m$ ) than that calculated from UV/VIS data (see figure 14). Since the two data sets were obtained simultaneously, this result is probably due to differences in the phenomena being measured, not to destabilization of the protein by the microwaves. Unfolding results from UV/VIS spectroscopy in the presence and absence of microwaves are identical within experimental error, indicating that the protein is not destabilized under the conditions used (data not shown).

#### 4. Future directions

To improve broadband stimulus-response measurements, both higher power systems and those with more array elements will be needed. Video-rate detection and imaging will depend on setting high enough offset frequencies between the coherent source and detector; this requires faster baseband processing.

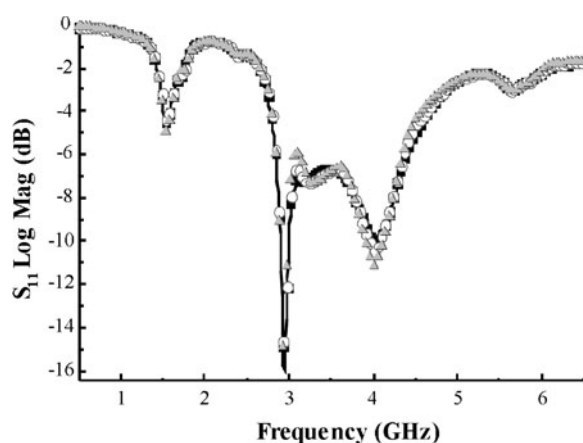


**Figure 13.** Spectral response of RNase-A solution to increasing temperature.

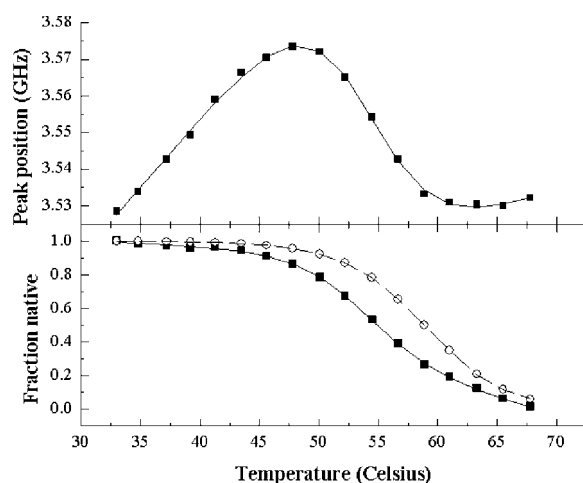


**Figure 14.** Raw data from peak shift (above); data fitted to unfolding theory and compared to UV-vis absorption (open circles, below).

To extend the protein solution experiments, we will perform additional unfolding at a variety of pH, concentration and microwave power conditions in order to detect limits of system and possible destabilization of the protein. Also needed are enzymology studies to ensure that activity of protein is unaffected. Other macromolecules might also be studied, such as DNA, RNA, carbohydrates and lipids. Finally, we will scale down the size of the experiment to move it higher in frequency.

## 5. Summary

We have discussed both broadband and resonant probing of biological samples and common powders using microwave and broadband systems. Broadband stimulus-response capabilities enable spectroscopic imaging, and increase the likelihood of sample identification, while experiments on purified and modulated samples demonstrate conclusively the use of water

bound to a protein as a label, and that the change of conformation can be observed in the perturbation of electric fields in the near zone of a slot antenna.

### Acknowledgments

This work was sponsored by the United States National Science Foundation, Office of Naval Research, Air Force Office of Scientific Research and Army Research Office. Earlier work on THz imaging was sponsored by the Federal Aviation Administration.

### References

- Akhavan H G and Mirshekar-Syahkal D 1999 *National Conference on Antennas and Propagation* vol 461, pp 8–11
- Bostak J S 1994 *Electrical Engineering* (Stanford: Stanford University) p 90
- Bostak J S, van der Weide D W, Bloom D M, Auld B A and Özbay E 1994 *J. Opt. Soc. Am. B* **11** 2561–5
- Bykhovskaia M, Gelmont B, Globus T, Woolard D L, Samuels A C, Duong T H and Zakrzewska K 2001 *Theor. Chem. Accounts* **106** 22–7
- Creighton T E 1993 *Proteins: Structures and Molecular Properties* (New York: Freeman)
- Facer G R, Notterman D A and Sohn L L 2001 *Appl. Phys. Lett.* **78** 996–8
- Feldman Y, Andrianov A, Polygalov E, Ermolina I, Romanychev G, Zuev Y and Milgotin B 1996 *Rev. Sci. Instrum.* **67** 3208–16
- Fitzgerald A J, Berry E, Zinovev N N, Walker G C, Smith M A and Chamberlain J M 2002 *Phys. Med. Biol.* **47** R67–R84
- Han P Y and Zhang X C 2000 *Laser Focus World* **36** 117
- Hefti J, Pan A and Kumar A 1999 *Appl. Phys. Lett.* **75** 1802–4
- Hollis M A, Blackman C F, Weil C M, Allis J W and Schaefer D J 1980 *IEEE Trans. Microw. Theory Tech.* **28** 791–801
- Kindt J T and Schmuttenmaer C A 1997 *J. Chem. Phys.* **106** 4389–400
- Klink T A, Woycechowsky K J, Taylor K M and Raines R T 2000 *Eur. J. Biochem.* **267** 566–72
- Konishi Y, Kamegawa M, Case M, Ruai Y, Allen S T and Rodwell M J W 1994 *IEEE Trans. Microw. Theory Tech.* **42** 1131–9
- Konishi Y, Kamegawa M, Case M, Yu R, Rodwell M J W and York R A 1992 *Appl. Phys. Lett.* **61** 2829–31
- Markelz A G, Roitberg A and Heilweil E J 2000 *Chem. Phys. Lett.* **320** 42–8
- Nandi N, Bhattacharyya K and Bagchi B 2000 *Chem. Rev.* **100** 2013–45
- Nuss M C and Orenstein J 1998 *Terahertz Time-Domain Spectroscopy: Millimeter Wave Spectroscopy of Solids* vol 74, ed G Gruener (New York: Springer) pp 7–50
- Pace C N, Grimsley G R, Thomas S T and Makhatadze G I 1999 *Protein Science* **8** 1500–4
- Pethig R 1979 *Dielectric and Electronic Properties of Biological Materials* (Chichester: Wiley)
- Pethig R 1992 *Annu. Rev. Phys. Chem.* **43** 177–205
- Rodwell M J W *et al* 1994 *Proc. IEEE* **82** 1035–59
- Rodwell M J W, Kamegawa M, Yu R, Case M, Carman E and Giboney K S 1991 *IEEE Trans. Microw. Theory Techniques* **39** 1194–204
- Segelstein D J 1981 The complex refractive index of water *MS Thesis* University of Missouri, Kansas City
- Sheen D M, McMakin D L and Hall T E 2001 *IEEE Trans. Microw Theory Tech.* **49** 1581–92
- Smye S W, Chamberlain J M, Fitzgerald A J and Berry E 2001 *Phys. Med. Biol.* **46** R101–R112
- Tama F, Gadea F X, Marques O and Sanejouand Y H 2000 *Proteins—Structure Function and Genetics* **41** 1–7
- Taylor K and van der Weide D W 2001a *Photonics Boston* vol 4574 (Boston, MA: SPIE) pp 137–43
- Taylor K and van der Weide D W 2001b *9th Int. Conf. on Terahertz Electronics (Charlottesville)*
- van der Weide D W 1994 *Appl. Phys. Lett.* **65** 881–3
- van der Weide D W, Bostak J S, Auld B A and Bloom D M 1991 *Electron. Lett.* **27** 1412–3
- van der Weide D W, Bostak J S, Auld B A and Bloom D M 1993 *Appl. Phys. Lett.* **62** 22–4
- Wichaidit C, Peck J R, Lin Z, Hamers R J, Hagness S C and van der Weide D W 2001 *IEEE MTT-S Int. Microwave Symp. Dig.* **1** 163–6